RAPID COMMUNICATIONS

PHYSICAL REVIEW A VOLUME 48, NUMBER 4 OCTOBER 1993

Ultracold photoassociative ionization collisions in a magneto-optical trap: The optical-field-intensity dependence in a radiatively dissipative environment

V. Bagnato,* L. Marcassa,* Y. Wang, and J. Weiner†
Department of Chemistry and Biochemistry, University of Maryland, College Park, Maryland 20742

P. S. Julienne
Molecular Physics Division, National Institute of Standards and Technology, Gaithersburg, Maryland 20899

Y. B. Band
Department of Chemistry, Ben-Gurion University, Beer Sheeva, Israel 84105
(Received 21 July 1993)

We report here measurements of two-body associative-ionization collisions between sodium atoms confined in a magneto-optic trap. These collisions represent a kind of "open" or dissipative collision for which the energy of the atom plus applied light field subsystem need not be conserved due to spontaneous-emission coupling to the vacuum modes of the radiation field. The experiment measures the photoassociative-ionization-rate constant as a function of the optical field intensity from about 40 to 260 mW cm^{-2}. These results are in reasonable agreement with the predictions of an optical-Bloch-equation theory [Y. B. Band and P. S. Julienne, Phys. Rev. A **46**, 330 (1992)], but differ strongly from the predictions of a local-equilibrium theory [A. Gallagher, Phys. Rev. A **44**, 4249 (1991)].

PACS number(s): 32.80.Pj

We report here studies of collisions between sodium atoms optically confined and cooled by the dissipative spontaneous-light force to temperatures well below T_s ($\simeq$65 mK for sodium), the point at which a collision duration becomes longer than the spontaneous-emission lifetime. Ultracold collisions involving excited states are truly novel because, at the extremely long time and distance scales inherent in this regime, radiative coupling and spontaneous decay become significant, and inelastic collision probabilities can be manipulated by intensity, frequency, and polarization of applied optical fields. Ultracold collisions represent a fundamentally new kind of low-pressure, gas-phase process—an "open" or dissipative one in which the fluctuating, stochastic force of spontaneous emission to the vacuum modes of the radiation field can result in energy nonconservation within the subsystem comprised of the colliding atoms plus applied laser field. Density-matrix methods rather than wave-function methods must be used to describe the collision, and crucial experimental tests are needed to develop an understanding of the collision dynamics. Such collisions serve as prototype and paradigm systems for studying the properties of nonequilibrium open systems coupled to reservoirs, e.g., conductance and transport in mesoscopic and macroscopic systems in which irreversibility is present.

Reports of atom optical cooling [1] inspired early calculations of photon-stimulated two-body association reactions [2], and the observation of associative ionization (AI) between optically cooled sodium atoms [3] demonstrated the ability to manipulate the inelastic rate constant with radiation field intensity. Recent experiments [4] sweeping the frequency of a dipole optical trap to $\simeq$4 GHz to the red side of the Na atomic resonance line have revealed structure in the AI production rate and have been interpreted [5] using a model that identifies the specific transient molecular states of the collision intermediate. Collisions in an optical trap are an important loss process limiting attainable density, and studies of total trap-loss rates [6,7] have confirmed the essentially molecular nature of photon absorption during the collisional encounter.

In this Rapid Communication we report measurements of the intensity dependence of the absolute rate constant for photoassociative ionization (PAI) in a magneto-optical trap (MOT) [8] and show that two theoretical approaches [9,10] based on different physical models of these "open" collisions predict rate coefficients that differ by an order magnitude. We adopt the term photoassociative ionization so as to distinguish the ultracold process from its familiar counterpart, associative ionization occurring at ordinary temperatures. Conventional AI proceeds in two distinct steps: excitation of isolated atoms followed by the collisional interaction between excited atomic states. The collision event is fast compared to radiative relaxation, and the two steps are decoupled. In contrast, PAI begins between *ground-state* partners moving sufficiently slowly that they have time to absorb and spontaneously emit photons prior to the final ionizing interaction. The partners must be in close enough proximity at the initial absorption that a significant fraction of the excited population survives relaxation back to the ground state. Thus PAI starts by promoting the ground state of the colliding species, designated Na··Na, to an intermediate excited molecular state at long range, designated [Na··Na]*. As the partners accelerate towards each other along the incoming trajectory, the excited quasimolecule absorbs a second photon to a doubly excited state, [Na··Na]**, which then proceeds to autoionize at close range,

$$\mathrm{Na}+\mathrm{Na}\rightarrow\mathrm{Na}\cdot\cdot\mathrm{Na}+h\nu\rightarrow[\mathrm{Na}\cdot\cdot\mathrm{Na}]^{*},$$
$$[\mathrm{Na}\cdot\cdot\mathrm{Na}]^{*}+h\nu\rightarrow[\mathrm{Na}\cdot\cdot\mathrm{Na}]^{**}\rightarrow\mathrm{Na}_2^{+}\ . \quad (1)$$

The rate of ion production is given by

$$d[\mathrm{Na}_2^{+}]/dt=k_{\mathrm{PAI}}[N]^2 \quad (2)$$

where $[\mathrm{Na}_2^{+}]$,$[N]$ are the ion and atom densities respectively and k_{PAI} is the rate constant [5,11].

Figure 1 shows a schematic of the experimental setup. Sodium vapor from an adjacent sidearm maintained at 350 K effuses through a leak value into the main chamber. The low-velocity tail of the thermal distribution loads into the MOT. A combination of turbomolecular and ion pumping maintains a background pressure below 10^{-6} Pa (10^{-8} torr). The magnetic-field coils, located external to the chamber, produce a field gradient of about 0.002 T cm^{-1} (20 G cm^{-1}) axially at the center of the trap and about 0.001 T cm^{-1} in the central transverse plane. Light from a ring dye laser is tuned about one linewidth to the red side of the $\mathrm{Na}(3s\ ^2S_{1/2};F=2)\rightarrow\mathrm{Na}(3p\ ^2P_{3/2};F=3)$ and introduced into the main chamber through ports along and orthogonal to the magnetic-field axis. The blue sideband, produced by a 1712-MHz electro-optic modulation of the carrier, excites the "repumping" transition $\mathrm{Na}(3s\ ^2S_{1/2};F=1)\rightarrow\mathrm{Na}(3p\ ^2P_{3/2};F=2)$ to prevent loss of trap population by unwanted optical pumping processes. Determination of the PAI rate constant requires accurate measurement of the trapped atom density and Na_2^{+} production rate. We obtain the density by imaging the bright fluorescent volume of the trap onto a calibrated photomultiplier tube (PMT) while measuring its dimensions ($\simeq$200 μm $\times$600 μm) with a telescope mounted on precision XY translation states. Reference [6] demonstrates that the radiation trapping properties of an optically thick cloud of trapped atoms results in an atomic ensemble of constant density. Careful scrutiny of the trapped-atom spatial distribution reveals an approximate oblate spheroid, but the detailed shape varies from run to run, introducing the dominant uncertainty in the rate constant measurement. Knowledge of the fluorescence rate f striking the PMT, the solid angle subtended, and the spatial extent of the trap determines the atom total number N through the relation

$$f=GN\frac{\rho_{22}}{\tau}=GN\frac{1}{2\tau}\frac{\Omega_0^2/2}{(\omega_0-\omega)^2+(\Gamma/2)^2+(\Omega_0^2/2)}, \quad (3)$$

where G is the photon collection efficiency, N the total number of atoms in the trap, ρ_{22} the fractional excited-state population, and τ, Γ, and Ω_0 the radiative lifetime, natural linewidth, and on-resonance Rabi frequency, respectively. We have used the on-resonance Rabi frequency calculated by Farrell, MacGillivray, and Standage [12] and entered in Table II of that paper. The small spatial extent of the trap (200 μm $\times$600 μm) compared to the width of the MOT laser beams (8 mm) insures negligible spatial variation of Ω_0 over the trap dimensions. The MOT performs optimally with a red detuning $\omega-\omega_0$ of about one linewidth, typically operating with a volume of approximately 8×10^{-5} cm^3 and a ground-state density of approximately 1×10^{10} cm^3. A Channeltron particle multiplier positioned 28 mm from the trap center and fitted with a negatively biased grid collects and counts the ions produced by PAI. Numerical simulation of the ion trajectories verifies unit collection efficiency onto the biased grid. Overall counting efficiency is therefore only limited by the opacity factor α (35%) of the collection grid. Count rates approximately equal to 200 sec^{-1} with a signal-to-noise ratio approximately equal to 15 typify usual conditions. The intensity-dependent rate constant $k_{\mathrm{PAI}}(I)$ for process (1) is then calculated from

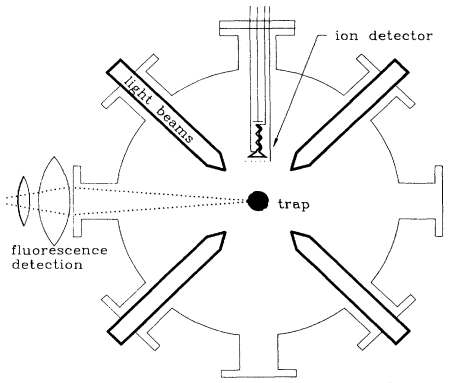

FIG. 1. Schematic diagram of the MOT. A pair of cooling laser beams counterpropagate on an axis perpendicular to the figure plane as well as the two pairs shown.

$$(1/V)[d(i/\alpha)/dt]=k_{\mathrm{PAI}}(I)[N]^2, \quad (4)$$

where V is the measured trap volume, and $d(i/\alpha)/dt$ the ion production rate. We determined effective field intensity I (mW cm^{-2}) by measuring the total power with a calibrated thermopile and subtracting the power appearing in the modulated sidebands. Closing the beamwidth to 63% of total power determines the spot size. Successive neutral density filters coated on a fixed wheel substrate permitted variation of I without disturbing the overall optical alignment.

The MOT operates with three frequencies present: a central "carrier" frequency tuned to the trap transition $^2S_{1/2}(F=2)\rightarrow{}^2P_{3/2}(F=2)$, a "repumper" sideband shifted 1712 MHz to the blue of the carrier, tuned to $^2S_{1/2}(F=1)\rightarrow{}^2P_{32}(F=2)$, and a second sideband shifted an equal interval to the red of the carrier. This "red" sideband is a consequence of electro-optic (EO) modulation and does not connect states of the isolated atoms. In normal MOT operation the intensity of each sideband is about 25% of the carrier's. In order to verify that the sidebands were not influencing the collisional process, we decreased the modulation efficiency of the EO by decoupling the radio frequency power from the EO crystal. We were able to decrease the sideband intensity, relative to that of the carrier, from 25 to 11 mW cm^{-2}. Reducing the repumper power changes the volume and density of the trap somewhat, but redetermination of the rate constant for PAI in the new trap conditions shows that, to within experimental uncertainty, sideband light has no effect on the photoassociative-ionization rate constant. Theoretical calculations of k_{PAI} also show that contribution from sideband frequencies should be negligible.

Figure 2 presents the results of the measurements of the absolute rate constants together with calculations

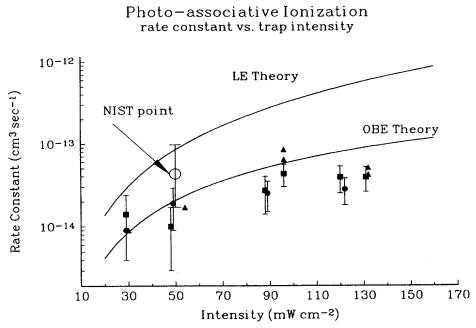

FIG. 2. Photoassociative-ionization rate constant vs MOT intensity. Different symbols indicate separate runs. Uncertainty in the determination of trap volume dominates the contribution to the error bars. The single filled circle is the result from the earlier measurement of Ref. [4]. Curves labeled OBE and LE are calculated from the optical-Bloch-equation theory of Ref. [10] and the local equilibrium theory of Ref. [9].

from two recent theories [9,10] of ultracold PAI. The experimental results reported here agree with a previous measurement of Lett *et al.* [4] within error bars. The semiclassical optical Bloch equation (OBE) theory, previously developed to treat trap-loss collisions [10], agrees well with the experimental results at the low end of the intensity scale, but the measured rate constants appear to "saturate" with increasing intensity sooner than theory. In contrast, the Gallagher local equilibrium (LE) theory [9] calculates a rate constant greater than experiment by about a factor of 8 at low intensity.

We have applied the OBE and LE theories using exactly the same molecular-state parameters, so any differences will be due to contrasting dynamical approximations. Reaction rates were calculated from the LE theory by numerical evaluation [14] of Eq. (9) of Ref. [9]. The molecular states of the model, taken from Ref. [5], are shown in Fig. 3. The interpretation of PAI dynamics is aided by defining the Condon point R_C, the distance at which the molecule is in resonance with the exciting light, that is, $V^*(R_C)-V(R_C)=\hbar\omega$ or $V^{**}(R_C)-V^*(R_C)=\hbar\omega$, where the molecular potentials V, V^*, and V^{**} refer to the states in Fig. 3. In normal, high-temperature collisions, the existence of a Condon point implies a region of stationary phase for evaluating the Franck-Condon overlap integral between upper and lower states. Transitions with Condon points typically have much more favorable Franck-Condon factors than those without, which are considered to be classically forbidden.

The first step in Eq. (1) is a transition from the ground $^3\Sigma_u^+$ state, Na··Na, having a flat van der Waals potential $V(R)$ for $R>1000a_0$, to attractive intermediate 0_g^- and 1_g molecular states. When the laser is tuned one atomic linewidth, $\hbar\Gamma$ with $\Gamma=2\pi(10\text{ MHz})$, to the red of resonance with the $^2S_{1/2}(F=2)\rightarrow{}^2P_{3/2}(F=3)$ hyperfine transition, the first step for exciting either the 0_g^- or 1_g molecular states, indicated on Fig. 3, has a Condon point near $R\approx 2000a_0$. The excited atoms then move together while being accelerated by the attractive $V^*(R)$ potential. The second step is excitation to a doubly excited molecular 1_u state, [Na··Na]**, which connects with a short-

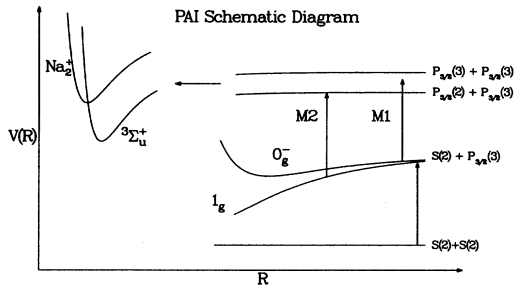

FIG. 3. Schematic (not to scale) diagram of the molecular pathways postulated in Ref. [5] to lead to PAI in a MOT, with MOT laser detuning of one atomic linewidth (10 MHz) to the red of the $^2S_{1/2}(F=2)\rightarrow{}^2P_{3/2}(F=3)$ transition. Two-step excitation transfers the population to the doubly excited 1_u state. The second step can proceed by either of two mechanisms, designated $M1$ and $M2$, depending on which atomic $P_{3/2}$ hyperfine component is excited: $M1$ is off resonant at all R, but $M2$ is resonant near $R=1000a_0$, since $R_{3/2}(F=2)$ lies 6 atomic linewidths below $P_{3/2}(F=3)$. Autoionization only occurs if the scattering flux reaches the short-range $^3\Sigma_u^+$ molecular state before spontaneous decay occurs.

range autoionizing $^3\Sigma_u^+$ state. PAI only occurs if the atoms come together on this doubly excited state, surviving decay by spontaneous emission before they reach $R\approx 10a_0$, where they autoionize. The second excitation step can occur by either of two mechanisms, which depend critically on the excited-state hyperfine structure. If the second step excites the upper $^2P_{3/2}(F=3)$ hyperfine component, indicated by $M1$ in Fig. 3, there is *no* Condon point, since the $V(R)^{**}$ potential is flat at long range and $V^*(R)$ is attractive, i.e., $V^{**}(R)-V^*(R)-\hbar\omega>\hbar\gamma\neq 0$. But if the second step excites the next lowest hyperfine level, $^2P_{3/2}(F=2)$, lying approximately $6\hbar\gamma$ below the first, there are Condon points for either the 0_g^- or 1_g intermediate states, indicated as $M2$ near $R\approx 1000a_0$ in Fig. 3. We have calculated the contributions of both mechanisms, $M1$ and $M2$, using the LE and OBE theories. The original LE theory [9] did not include $M2$.

The calculation of k_{PAI} in Eq. (2) by either the OBE or LE theories requires determining two probabilities: first, the probability P_{ES} that the multistep excitation-survival process described above brings the two excited atoms together near $R\approx 10a_0$ on the autoionizing molecular $^3\Sigma_u^+$ state; second, the probability P_{AI} of autoionization, given the atoms are colliding along the $^3\Sigma_u^+$ state near $R\approx 10a_0$. This second probability is common to both theories. Our choice of P_{AI}, described in detail in Ref. [10], is 2.7 times larger than the original choice of Gallagher, due to different assumptions about how to infer this ionizing probability in the ultracold regime from measurements carried out under conventional conditions [15]. At least a factor of 2 uncertainty must still be attached to this parameter, so any theory of PAI must be considered uncertain by at least this amount.

The LE and OBE theories differ widely in the methods and physical assumptions used to calculate P_{ES}. The OBE method calculates P_{ES} by propagating a density matrix for the molecular populations and coherences from

equilibrium at large R into $R=10a_0$, including laser optical-field dressing of the molecular states participating in the dynamics, and population and coherence decay due to spontaneous emission. The relative motion of the atoms is treated semiclassically with WKB-like corrections for the time-dependent relative motion of the atoms in the various channels. These corrections account for the widely different trajectories in the ground and excited states. Thus, cross sections can be calculated in a manner that is independent of the choice of the reference trajectory used to propagate the equations [10]. In the LE theory step 1 occurs from a quasistatic distribution of stationary atoms at some distance R. The atoms accelerate on $V^*(R)$ from zero initial velocity at R to velocity $v(R')$ at R', then absorb a second photon to the doubly excited state at R', and continue to evolve on $V^{**}(R)$ with initial velocity $v(R')$. The probability of spontaneous decay during the motion is calculated semiclassically. The excitation line shapes are R-dependent Lorentzians, peaking at a Condon point but permitting *nonresonant* excitation away from a Condon point. The probability P_{ES} results from integrating over all R and R'. The LE model is in accord with the classical Franck-Condon principal (CFCP); i.e., velocity remains unchanged after a transition "occurs" at some distance R or R'.

In the conventional theory of collisions in a radiation field [16], the total energy of the final scattering state is completely prescribed by the usual energy conservation condition, $E=E_i+\hbar\omega$ for one-photon and $E_i+2\hbar\omega$ for two-photon transitions. These conditions define the "on-the-energy-shell" kinetic energy for each channel at each R. In the dissipative environment of an ultracold excited-state collision, local kinetic energy need not satisfy such a condition [10], and "off-the-energy-shell" trajectories can contribute to the dynamics. But Smith, Burnett, and Julienne [17] use a semiclassical WKB analysis to argue that excited-state trajectories should stay close to remaining "on the energy shell." In the LE theory off-resonant excitation at distances away from Condon points plays a crucial role, and the second step need not be resonant. Thus, mechanisms $M1$ and $M2$ above both contribute significantly to PAI in the LE theory. Using the CFCP for off-resonant excitation in the LE theory picks excited-state trajectories that are "off the energy shell." In the OBE theory, excited-state trajectories remain close to "on the energy shell." Also, off-resonant excitation is strongly suppressed in the OBE theory because of quantum oscillations in the coherence terms that drive the populations, and the contribution from mechanism $M1$, which has no Condon point in the second step, is negligible in comparison to that of mechanism $M2$, which does have a Condon point. Therefore, the OBE calculations support the conclusion of Ref. [5] that the excited-state hyperfine structure plays a critical role in enhancing the PAI rate for MOT conditions.

Both the LE and semiclassical OBE theory are approximate theories based on very different physical pictures of the ultracold dynamics. The present experiment indicates that the LE theory seriously overestimates the PAI rate coefficient for MOT conditions. Full quantum density-matrix wave-packet methods are being developed to improve these semiclassical models, although such calculations are just barely feasible with present computers. The OBE and LE theories make very different predictions concerning the variation of PAI rate with detuning and temperature, and experiments to test these are planned. Understanding the collision dynamics modified by excited-state decay is crucial for interpreting these "open" quantum collisions. It is very important to continue development of both theory and experiment to resolve the many fundamental issues raised by these unique ultracold collisions.

V.B. and L.M. acknowledge financial support from "Fundacaõ de Amparo a Pesquisa do Estado de São Paulo" (FAPESP) and CNPQ. J.W. acknowledges support from the National Science Foundation and the National Institute of Standards and Technology. Acknowledgment is also made of the Donors of the Petroleum Research Fund, administered by the American Chemical Society, for partial support of this research. P.J. and Y.B. acknowledge partial support from the Office of Naval Research.

*Permanent address: Instituto de Física e Química de São Carlos–USP, Cx. Postal 369, 13560 São Carlos, SP, Brazil.

†Present address: Physics Division, National Science Foundation, 1800 G Street, NW, Washington DC 20550.

[1] For accounts of early work on optical cooling, trapping, and ultracold collisions, see *The Mechanical Effects of Light,* special issue of J. Opt. Soc. Am. B **2**, 1706 (1985); and *Laser Cooling and Trapping of Atoms,* special issue of J. Opt. Soc. Am. B **6**, 2020 (1989).

[2] H. R. Thorsheim *et al.*, Phys. Rev. Lett. **58**, 2820 (1987).

[3] P. L. Gould *et al.*, Phys. Rev. Lett. **60**, 788 (1988).

[4] P. D. Lett *et al.*, Phys. Rev. Lett. **67**, 2139 (1991).

[5] P, S. Julienne and R. Heather, Phys. Rev. Lett. **67**, 2135 (1991); R. Heather and P. S. Julienne, Phys. Rev. A **47**, 1887 (1993).

[6] D. Hoffmann *et al.*, Phys. Rev. Lett. **69**, 753 (1992), and references cited therein.

[7] C. D. Wallace *et al.*, Rev. Lett. **69**, 897 (1992).

[8] E. L. Raab *et al.*, Phys. Rev. Lett. **59**, 2631 (1987).

[9] A. Gallagher, Phys. Rev. A **44**, 4249 (1991).

[10] Y. B. Band and P. S. Julienne (unpublished).

[11] Note that this definition differs from that of Gallagher in that a homonuclear symmetry factor of 2 is included in the definition of k_{PAI} rather than with the density product $N^2/2$.

[12] P. M. Farrell *et al.*, Phys. Rev. A **37**, 4240 (1988).

[13] Y. B. Band and P. S. Julienne, Phys. Rev. A **46**, 330 (1992).

[14] We were unable to reproduce numerically Fig. 7 of Ref. [9], although we fully agree with the analytic formulas of Eq. (9) and those following. Note also that the quantity $\gamma h\omega_0/\lambda^2$ has a magnitude of 76 mW/cm^2 rather than 6 mW/cm^2 when the parameters of Ref. [9] are used.

[15] J. Huennekens and A. Gallagher, Phys. Rev. A **28**, 1276 (1983); R. Bonanno, J. Boulmer, and J. Weiner, *ibid.* **28**, 604 (1983); H. A. J. Meijer, Z. Phys. D **17**, 257 (1990).

[16] P. S. Julienne and F. H. Mies, Phys. Rev. A **30**, 831 (1984).

[17] A. M. Smith *et al.*, Phys. Rev. A **46**, 4091 (1992).